

Polarization Transfer in Proton Compton Scattering at High Momentum Transfer

D. J. Hamilton,¹ V. H. Mamyan,^{2,3} K. A. Aniol,⁴ J. R. M. Annand,¹ P. Y. Bertin,⁵ L. Bimbot,⁶ P. Bosted,⁷ J. R. Calarco,⁸ A. Camsonne,⁵ G. C. Chang,⁹ T.-H. Chang,¹⁰ J.-P. Chen,³ Seonho Choi,¹¹ E. Chudakov,³ A. Danagoulian,¹⁰ P. Degtyarenko,³ C. W. de Jager,³ A. Deur,¹² D. Dutta,¹³ K. Egiyan,² H. Gao,¹³ F. Garibaldi,¹⁴ O. Gayou,¹⁵ R. Gilman,^{3,16} A. Glamazdin,¹⁷ C. Glashauser,¹⁶ J. Gomez,³ J.-O. Hansen,³ D. Hayes,¹⁸ D. Higinbotham,³ W. Hinton,¹⁸ T. Horn,⁹ C. Howell,¹³ T. Hunyady,¹⁸ C. E. Hyde-Wright,¹⁸ X. Jiang,¹⁶ M. K. Jones,³ M. Khandaker,¹⁹ A. Ketikyan,² V. Koubarovski,²⁰ K. Kramer,¹⁵ G. Kumbartzki,¹⁶ G. Laveissière,⁵ J. LeRose,³ R. A. Lindgren,¹² D. J. Margaziotis,⁴ P. Markowitz,²¹ K. McCormick,¹⁸ Z.-E. Meziani,¹¹ R. Michaels,³ P. Moussiegt,²² S. Nanda,³ A. M. Nathan,¹⁰ D. M. Nikolenko,²³ V. Nelyubin,²⁴ B. E. Norum,¹² K. Paschke,⁷ L. Pentchev,¹⁵ C. F. Perdrisat,¹⁵ E. Piasetzky,²⁵ R. Pomatsalyuk,¹⁷ V. A. Punjabi,¹⁹ I. Rachek,²³ A. Radyushkin,^{3,18} B. Reitz,³ R. Roche,²⁶ M. Roedelbronn,¹⁰ G. Ron,²⁵ F. Sabatie,¹⁸ A. Saha,³ N. Savvinov,⁹ A. Shahinyan,² Y. Shestakov,²³ S. Širca,²⁷ K. Slifer,¹¹ P. Solvignon,¹¹ P. Stoler,²⁰ S. Tajima,¹³ V. Sulkosky,¹⁵ L. Todor,¹⁸ B. Vlahovic,²⁸ L. B. Weinstein,¹⁸ K. Wang,¹² B. Wojtsekhowski,³ H. Voskanyan,² H. Xiang,²⁷ X. Zheng,²⁷ and L. Zhu²⁷

(The Jefferson Lab Hall A Collaboration)

¹University of Glasgow, Glasgow G12 8QQ, Scotland, U.K.

²Yerevan Physics Institute, Yerevan 375036, Armenia

³Thomas Jefferson National Accelerator Facility, Newport News, VA 23606

⁴California State University Los Angeles, Los Angeles, CA 90032

⁵Université Blaise Pascal/IN2P3, F-63177 Aubière, France

⁶IPN Orsay B.P. n° 1 F-91406, Orsay, France

⁷University of Massachusetts, Amherst, MA 01003

⁸University of New Hampshire, Durham, NH 03824

⁹University of Maryland, College Park, MD 20742

¹⁰University of Illinois, Urbana-Champaign, IL 61801

¹¹Temple University, Philadelphia, PA 19122

¹²University of Virginia, Charlottesville, VA 22901

¹³Duke University and TUNL, Durham, NC 27708

¹⁴INFN, Sezione di Sanità and Institute Superiore di Sanità, I-00161 Rome, Italy

¹⁵College of William and Mary, Williamsburg, VA 23187

¹⁶Rutgers, The State University of New Jersey, Piscataway, NJ 08854

¹⁷Kharkov Institute of Physics and Technology, Kharkov 61108, Ukraine

¹⁸Old Dominion University, Norfolk, VA 23529

¹⁹Norfolk State University, Norfolk, VA 23504

²⁰Rensselaer Physics Institute, Troy, NY 12180

²¹Florida International University, Miami, FL 33199

²²Institut des Sciences Nucleaires, CNRS-IN2P3, F-38016 Grenoble, France

²³Budker Institute for Nuclear Physics, Novosibirsk 630090, Russia

²⁴St. Petersburg Nuclear Physics Institute, Gatchina, 188350, Russia

²⁵Tel Aviv University, Tel Aviv 69978, Israel

²⁶Florida State University, Tallahassee, FL 32306

²⁷Massachusetts Institute of Technology, Cambridge, MA 02139

²⁸North Carolina Central University, Durham, NC 27707

(Dated: November 19, 2018)

Compton scattering from the proton was investigated at $s = 6.9 \text{ GeV}^2$ and $t = -4.0 \text{ GeV}^2$ via polarization transfer from circularly polarized incident photons. The longitudinal and transverse components of the recoil proton polarization were measured. The results are in excellent agreement with a prediction based on a reaction mechanism in which the photon interacts with a single quark carrying the spin of the proton and in disagreement with a prediction of pQCD based on a two-gluon exchange mechanism.

PACS numbers: 13.60.Fz, 24.85.+p

Real Compton Scattering (RCS) from the nucleon with s , $-t$, and $-u$ values large compared to Λ_{QCD}^2 is a hard exclusive process which provides access to information about nucleon structure complementary to high Q^2 elas-

tic form factors [1, 2] and Deeply Virtual Compton Scattering [3]. A common feature of these reactions is a high energy scale, leading to factorization of the scattering amplitude into a hard perturbative amplitude, which de-

scribes the coupling of the external particles to the active quarks, and the overlap of soft nonperturbative wave functions.

Various theoretical approaches have been applied to RCS in the hard scattering regime, and these can be distinguished by the number of active quarks participating in the hard scattering subprocess, or equivalently, by the mechanism for sharing the transferred momentum among the constituents. Two extreme pictures have been proposed. In the perturbative QCD (pQCD) approach (Fig. 1a) [4, 5, 6, 7], three active quarks share the transferred momentum by the exchange of two hard gluons. In the handbag approach (Fig. 1b)[8, 9, 10, 11], there is only one active quark whose wave function has sufficient high-momentum components for the quark to absorb and re-emit the photon. In any given kinematic regime, both mechanisms will contribute, in principle, to the cross section. It is generally believed that at sufficiently high energies, the pQCD mechanism dominates. However, the question of how high is “sufficiently high” is still open, and it is not known with any certainty whether the pQCD mechanism dominates in the kinematic regime that is presently accessible experimentally.

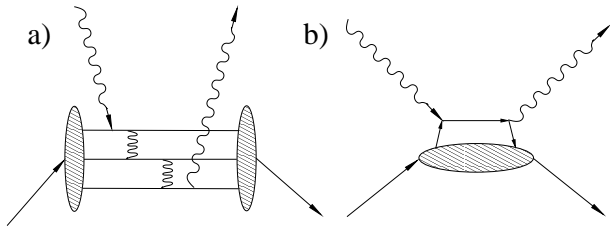


FIG. 1: RCS diagrams for the (a) pQCD and (b) handbag reaction mechanism.

One prediction of the pQCD mechanism for RCS is the constituent scaling rule [12], whereby $d\sigma/dt$ scales as s^{-6} at fixed θ_{CM} . The only data in the few GeV regime from the pioneering experiment at Cornell [13] are approximately consistent with constituent scaling, albeit with modest statistical precision. Nevertheless, detailed calculations show that the pQCD cross section underpredicts the data by factors of at least ten [6], thereby calling into question the applicability of the pQCD mechanism in this energy range. On the other hand, more recent calculations using the handbag approach have reproduced the Cornell cross-section data to better than a factor of two [8, 9]. The purpose of the present experiment [14] was to provide a more stringent test of the reaction mechanism by improving significantly on the statistical precision of the Cornell data, by extending those data over a broader kinematic range, and by measuring the polarization transfer observables K_{LL} and K_{LS} at a single kinematic point. The results of the latter measurements are reported in this Letter. As will be shown subsequently, these results are in unambiguous agreement

with the handbag mechanism and in disagreement with the pQCD mechanism.

The present measurement, shown schematically in Fig. 2, was carried out in Hall A at Jefferson Lab, with basic instrumentation described in [15]. A longitudinally-polarized, 100% duty-factor electron beam with current up to $40 \mu\text{A}$ and energy of 3.48 GeV was incident on a Cu radiator of 0.81 mm thickness. The mixed beam of electrons and bremsstrahlung photons was incident on a 15-cm liquid H_2 target, located just downstream of the radiator, with a photon flux of up to 2×10^{13} equivalent quanta/s. Quasi-real photons, which contribute 16% of total events with an average virtuality of 0.005 GeV^2 , were treated as a part of the RCS event sample. For incident photons at a mean energy of 3.22 GeV, the scattered photon was detected at a mean scattering angle of 65° in a calorimeter consisting of an array of 704 lead-glass blocks subtending a solid angle of 30 msr and with angular resolution of 1.8 mrad and relative energy resolution of 7.7%. The associated recoil proton was detected in one of the Hall A High Resolution Spectrometers (HRS) at the corresponding central angle of 20° and central momentum of 2.94 GeV. The HRS had a solid angle of 6.5 msr, momentum acceptance of $\pm 4.5\%$, relative momentum resolution of 2.5×10^{-4} , and angular resolution of 2.4 mrad, the latter limited principally by scattering in the target. The trigger was formed from a coincidence between a signal from a scintillator counter in the HRS focal plane and a signal above a 500 MeV threshold in the calorimeter. In total, 15 C and 3.5 C of beam charge were accumulated for RCS production and calibration runs, respectively.

Potential RCS events were selected based on the kinematic correlation between the scattered photon and the recoil proton. The excellent HRS optics was used to reconstruct the momentum, direction, and reaction vertex of the recoil proton and to calculate δx and δy , the difference in x and y coordinates, respectively, between the expected and measured location of the detected photon on the front face of the calorimeter. The distribution of events in δx with a coplanarity cut of $|\delta y| \leq 10 \text{ cm}$ is shown in Fig. 3. The RCS events, which are in the peak at $\delta x = 0$, lie upon a continuum background primarily from the $p(\gamma, \pi^0 p)$ reaction, with the subsequent decay $\pi^0 \rightarrow \gamma\gamma$. An additional background is due to electrons from ep elastic scattering, which is kinematically indistinguishable from RCS. A magnet between the target and the calorimeter (see Fig. 2) deflected these electrons horizontally by $\sim 20 \text{ cm}$ relative to undeflected RCS photons.

The recoil proton polarization was measured by the focal plane polarimeter (FPP) located in the HRS. The FPP determines the two polarization components normal to the momentum of the proton by measuring the azimuthal asymmetries in the angular distribution after scattering the proton from an analyzer, then taking the difference of these asymmetries between plus and minus

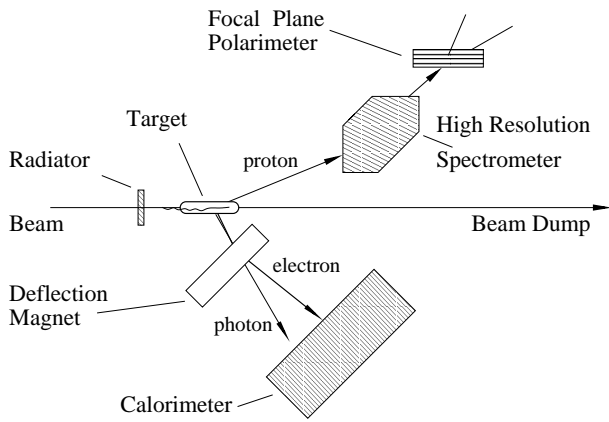


FIG. 2: Schematic layout of the RCS experiment.

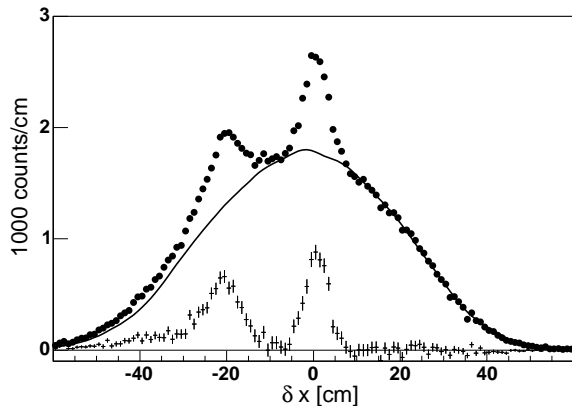


FIG. 3: Distribution of events in δx (points) with a coplanarity cut $|\delta y| \leq 10$ cm. The RCS and ep elastic events form the peaks at $\delta x = 0$ and -20 cm, respectively, and the photo-pion events the underlying continuum. A Monte Carlo simulation of the latter events is indicated by the solid curve. The difference between the data and simulation is shown by the points with uncertainties.

electron beam helicity states. To improve the efficiency, two analyzers were utilized in the experiment, a 44-cm block of CH_2 and a 50-cm block of carbon. Vertical drift chambers together with front and rear straw chambers tracked the protons before, between, and after the analyzers, effectively producing two independent polarimeters with a combined product of efficiency and square of analyzing power that was measured to be 4.5×10^{-3} . For each analyzer separately, Fourier analysis of the helicity difference leads to the product of the proton polarizations at the FPP (P_n^{fpp} or P_t^{fpp}), the circular polarization of the incident photon beam (P_γ^c), and the FPP analyzing power (A_y):

$$N(\vartheta, \varphi) = N_0(\vartheta) \left\{ 1 + \left[P_\gamma^c A_y(\vartheta) P_t^{fpp} + \alpha \right] \sin \varphi - \left[P_\gamma^c A_y(\vartheta) P_n^{fpp} + \beta \right] \cos \varphi \right\},$$

where N_0 is the number of protons which scatter in the polarimeter, ϑ and φ are the polar and azimuthal scatter-

ing angles, and α, β are instrumental asymmetries. Determination of $A_y(\vartheta)$, α , and β for each analyzer was performed by measuring the polarization of the recoil proton from $\bar{e}p$ elastic scattering at approximately the same momentum and by using previously determined ratio of the proton form factors [2]. The electron beam polarization was measured to be 0.766 ± 0.026 at the start of the experiment using a Møller polarimeter and continuously monitored throughout the production runs by observing the asymmetry due to the large $p(\gamma, \pi^0 p)$ background. An upper limit of 2% for the change of the beam polarization during the experiment was obtained from the pion data. The bremsstrahlung photon has 99% of the initial electron polarization over the energy range used [16].

To relate the proton polarization components at the focal plane to their counterparts at the target, the precession of the proton spin in the HRS magnetic elements was taken into account using a COSY model [17] of the HRS optics for the spin transport matrix. The elements of this matrix depend on the total precession angle, which was near 270° in order to optimize the determination of K_{LL} . The proton spin vector was then transformed to the proton rest frame, with the longitudinal axis pointing in the direction of the recoil proton in the center of mass frame [9]. In that frame, the longitudinal and transverse components of the proton polarization are just the spin transfer parameters K_{LL} and K_{LS} , respectively.

The RCS events are selected from a small elliptical region at the origin of the $\delta x - \delta y$ plane. For each spin component, the RCS recoil polarization is given by

$$P_{RCS} = [P_{all} - (1 - R)P_{bkg}] / R,$$

where P_{all} and P_{bkg} are the polarizations for all events and background events in that region, respectively, and R is the ratio of RCS to total events. The background polarization was measured by selecting events from regions of the $\delta x - \delta y$ plane that contain neither RCS nor ep elastic events. It was determined that within the statistical precision of the measurements, P_{bkg} was constant over broad regions of that plane. Results obtained with the two polarimeters were statistically consistent and were averaged. With the RCS region selected to obtain the best accuracy on P_{RCS} , one finds $R = 0.383 \pm 0.004$ and the resulting polarizations are given in Table I.

TABLE I: Proton recoil polarizations. For the RCS polarization the first uncertainty is statistical; the second is systematic and dominated by the background subtraction.

	P_{all}	P_{bkg}	$P_{RCS} = K_{LL} (K_{LS})$
LL	0.588 ± 0.030	0.532 ± 0.006	$0.678 \pm 0.083 \pm 0.04$
LS	0.340 ± 0.029	0.480 ± 0.006	$0.114 \pm 0.078 \pm 0.04$

The result for K_{LL} is shown in Fig. 4 along with the

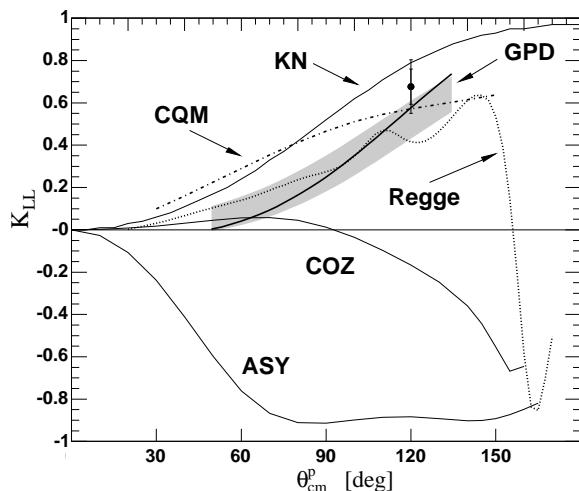


FIG. 4: Our result for K_{LL} compared with calculations in different approaches: ASY and COZ both from pQCD [7], GPD [10], CQM [11], and extended Regge model [18]. The curve labeled KN is K_{LL}^{KN} , the Klein-Nishina asymmetry for a structureless proton.

results of relevant calculations. In the handbag calculation using Generalized Parton Distributions (GPD),

$$K_{LL} \simeq \frac{R_A}{R_V} K_{LL}^{KN} \left[1 - \frac{t^2}{2(s^2+u^2)} \left(1 - \frac{R_A^2}{R_V^2} \right) \right]^{-1}$$

where R_A, R_V are axial and vector form factors, respectively, that are unique to the RCS process [9]. The experimental result implies the ratio $R_A/R_V = 0.81 \pm 0.11$.

The excellent agreement between the experiment and the GPD-based calculation, shown with a range of uncertainties due to finite mass corrections [19], and the close proximity of each to K_{LL}^{KN} are consistent with a picture in which the photon scatters from a single quark whose spin is in the direction of the proton spin. The RCS form factors are certain moments of the GPD's H and \tilde{H} [8, 9], so our result provides a constraint on relative values of these moments. An alternative handbag-type approach using constituent quarks (CQM) [11], with parameters adjusted to fit G_E^p data [2], is also in excellent agreement with the datum. Also in good agreement is a semi-phenomenological calculation using the extended Regge model [18], with parameters fixed by a fit to high- t photoproduction of vector mesons. On the other hand, the pQCD calculations [7], shown for both the asymptotic (ASY) and the COZ [20] distribution amplitude, disagree strongly with the experimental point, suggesting that the asymptotic regime has not yet been reached.

A non-zero value of K_{LS} implies a proton helicity-flip process, which is strictly forbidden in leading-twist pQCD. In the GPD-based approach [10], $K_{LS}/K_{LL} \simeq (\sqrt{-\hat{t}}/2M)R_T/R_V$, where \hat{t} is the four-momentum transfer in the hard subprocess of the handbag diagram, M is the proton mass, and R_T is a tensor form factor of the

RCS process. From the experimental result for K_{LS} , we estimate $R_T/R_V = 0.21 \pm 0.11 \pm 0.03$, where the first uncertainty is statistical and the second is systematic due to the mass correction uncertainty in calculating \hat{t} [19]. A value of 0.33 was predicted for R_T/R_V [10] based on the hypothesis $R_T/R_V = F_2/F_1$, the ratio of the Dirac and the Pauli electromagnetic form factors. Although the uncertainties are large, the present data suggest that R_T/R_V may fall more rapidly with $-t$ than F_2/F_1 . K_{LS} vanishes in the CQM-based handbag calculation [11].

In conclusion, the polarization transfer observables K_{LL} and K_{LS} were measured for proton Compton scattering in the wide-angle regime at $s = 6.9$, $t = -4.0$ GeV² and shown to be in good agreement with calculations based on the handbag reaction mechanism [10, 11].

We thank the Jefferson Lab Hall A technical staff for their outstanding support. This work was supported in part from the National Science Foundation, the UK Engineering and Physical Science Research Council, and the DOE under contract DE-AC05-84ER40150 Modification No. M175, under which the Southeastern Universities Research Association (SURA) operates the Thomas Jefferson National Accelerator Facility.

-
- [1] L. Andivahis *et al.*, *Phys. Rev. D* **50**, 5491 (1994).
 - [2] O. Gayou *et al.*, *Phys. Rev. Lett.* **88**, 092301 (2002).
 - [3] A. Airapetian *et al.*, *Phys. Rev. Lett.* **87**, 182001 (2001); S. Stepanyan *et al.*, *Phys. Rev. Lett.* **87**, 182002 (2001).
 - [4] G. P. Lepage and S. J. Brodsky, *Phys. Rev. D* **22**, 2157 (1980).
 - [5] G. R. Farrar and H. Zhang, *Phys. Rev. Lett.* **65**, 1721 (1990), *Phys. Rev. D* **42**, 3348 (1990).
 - [6] A. S. Kronfeld and B. Nizic, *Phys. Rev. D* **44**, 3445 (1991); M. Vanderhaeghen, P. A. M. Guichon and J. Van de Wiele, *Nucl. Phys. A* **622**, 144c (1997).
 - [7] T. Brooks and L. Dixon, *Phys. Rev. D* **62**, 114021 (2000).
 - [8] A. V. Radyushkin, *Phys. Rev. D* **58**, 114008 (1998).
 - [9] M. Diehl, T. Feldmann, R. Jakob, P. Kroll, *Eur. Phys. J. C* **8**, 409 (1999);
 - [10] H. W. Huang, P. Kroll, T. Morii, *Eur. Phys. J. C* **23**, 301 (2002), *Erratum ibid.*, **C 31**, 279 (2003); H. W. Huang, private communication.
 - [11] G. A. Miller, *Phys. Rev. C* **69**, 052201(R) (2004).
 - [12] S. J. Brodsky and G. Farrar, *Phys. Rev. Lett.* **31**, 1153 (1973); V. A. Matveev, R. M. Muradyan, and A. V. Tavkhelidze, *Lett. Nuovo Cimento* **7**, 719 (1973).
 - [13] M. A. Shupe *et al.*, *Phys. Rev. D* **19**, 1921 (1979).
 - [14] C. Hyde-Wright, A. Nathan, and B. Wojtsekhowski, spokespersons, JLab experiment E99-114.
 - [15] J. Alcorn *et al.*, *Nucl. Inst. Meth. A* **522**, 294 (2004).
 - [16] H. Olsen and L.C. Maximon, *Phys. Rev.* **114**, 887 (1959).
 - [17] K. Makino and M. Berz, *Nucl. Instr. Meth. A* **427**, 338 (1999).
 - [18] F. Cano and J. M. Laget, *Phys. Lett. B* **551**, 317 (2003).
 - [19] M. Diehl *et al.*, *Phys. Rev. D* **67**, 037502 (2003).
 - [20] V. L. Chernyak *et al.*, *Z. Phys. C* **42**, 569 (1989).